CHAPTER-3

THERMAL RADIATION AND ROTATION EFFECT ON AN UNSTEADY MHD MIXED CONVECTION FLOW THROUGH A POROUS MEDIUM WITH HALL CURRENT AND HEAT ABSORPTION

3.1 INTRODUCTION

The study of flow in rotating porous media is motivated by its practical applications in geophysics and engineering. Among the applications of rotating flow in porous media to engineering disciplines, one can find the food processing industry, chemical process industry, centrifugation filtration processes and rotating machinery. Also the hydrodynamic rotating flow of electrically conducting viscous incompressible fluids has gained considerable attention because of its numerous applications in physics and engineering. In geophysics, it is applied to measure and study the positions and velocities with respect to a fixed frame of reference on the surface of earth, which rotate with respect to an inertial frame in the presence of its magnetic field. The subject of geophysical dynamics now – a – days has become an important branch of fluid dynamics due to the increasing interest to study environment. In astrophysics, it is applied to study the stellar and solar structure, inter planetary and inter stellar matter, solar storms etc. In engineering, it finds its application in MHD generators, ion propulsion, MHD bearings, MHD pumps MHD boundary layer control of reentry vehicles etc. Several scholars viz. Crammer and Pai [6], Ferraro and Plumpton [7], Shercliff [20] have studied such flows because of their varied importance. MHD channel or duct flows are important from its practical point of view. Chang and Lundgren [4] have studied a hydromagnetic flow in a duct. Yen and Chang [26] analyzed the effect of wall electrical conductance on the magnetohydrodynamic Couette flow. From the technological point of view and due to practical applications, free convective flow and heat transfer problems are always important. This process of heat transfer is encountered in cooling of nuclear reactors, providing heat sinks in turbine blades and aeronautics. Ostrach [15] studied the combined effects of natural and forced convection laminar flow and heat transfer of fluids with and without heat sources in channels with linearly varying wall temperature. Jain and Gupta [10] studied three dimensional free convection Couette flow with transpiration cooling.

There are numerous important engineering and geophysical applications of the channel flows through porous medium, for example in the fields of agricultural engineering for channel irrigation and to study the underground water resources, in petroleum technology

to study the movement of natural gas, oil and water through the oil channels/reservoirs. Transient natural convection between two vertical walls with a porous material having variable porosity has been studied by Paul *et al.* [16]. Sahin [18] investigated the three – dimensional free convective channel flow through porous medium. Israel Cookey et al. [9] investigated the influence of viscous dissipation and radiation on unsteady MHD free convection flow past an infinite heated vertical plate in a porous medium with time dependent suction. Chamkha [3] investigated unsteady convective heat and mass transfer past a semi-infinite permeable moving plate with heat absorption where it was found that increase in solutal Grashoff number enhanced the concentration buoyancy effects leading to an increase in the velocity.

In recent years, the effects of transversely applied magnetic field on the flows of electrically conducting viscous fluids have been discussed widely owing to their astrophysics, geophysical and engineering applications. Attia and Kotb [2] studied MHD flow between two parallel plates with heat transfer. When the strength of the magnetic field is strong, one cannot neglect the effects of Hall current. The rotating flow of an electrically conducting fluid in the presence of a magnetic field is encountered in geophysical and cosmical fluid dynamics. It is also important in the solar physics involved in the sunspot development. Soundalgekar *et.al* [25] studied the Hall effects in MHD Couette flow with heat transfer. Mazumder *et al* [11, 12] have studied the effects of Hall current on MHD Ekman layer flow and heat transfer over porous plate and on free and forced convective hydromagnetic flow through a channel. Hall effects on unsteady MHD free and forced convection flow in a porous rotating channel has been investigated by Sivaprasad *et al.* [24]. Singh and Kumar [21] studied the combined effects of Hall current and rotation on free convection MHD flow in a porous channel. Ghosh *et al.* [8] studied the Hall effects on MHD flow in a rotating system with heat transfer characteristics. Satyanarayana and Venkataramana [19] studied Hall current effect on magnetohydrodynamics free-convection flow past a semi infinite vertical porous plate with mass transfer.

Radiative convective flows have gained attention of many researchers in recent years. Radiation plays a vital role in many engineering, environment and industrial processes

e.g. heating and cooling chambers, fossil fuel combustion energy processes astrophysical flows and space vehicle re – entry. Raptis [17] studied the radiation and free convection flow through a porous medium. Alagoa *et al* [1] analyzed the effects of radiation on free convective MHD flow through a porous medium between infinite parallel plates in the presence of time – dependent suction. Mebine [13] studied the radiation effects on MHD Couette flow with heat transfer between two parallel plates. Singh and Kumar [22] have studied radiation effects on the exact solution of free convective oscillatory flow through porous medium in a rotating vertical porous channel.

The main objective of the present chapter is to study the MHD free convective flow in a rotating channel filled with porous medium with Hall current and heat absorption in the presence of viscous dissipation. The resulting non-dimensional governing equations are solved by Galerkin finite element method. Numerical results are obtained for velocity, temperature, skin friction, and Nusselt numbers for various values of parameters occurring in the problem and are presented in the graphical form. The transverse magnetic field applied is strong enough so that the Hall currents are induced. The temperature difference between the walls of channel is sufficiently high to radiate the heat.

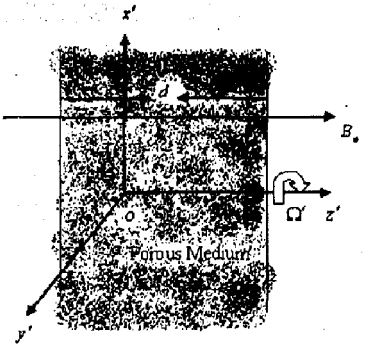

Figure 1.Schematic diagram of the physical problem

BASIC EQUATIONS

The equations governing the unsteady free convective flow of an incompressible, viscous and electrically conducting fluid in a rotating vertical channel filled with porous medium in the presence of magnetic field are:

Equation of Continuity:

$$div\,\bar{V} = 0 \tag{1}$$

Momentum Equation:

$$\rho\left[\frac{\partial \bar{V}}{\partial t'} + \bar{\Omega}\times\bar{V} + (\bar{V}.\nabla)\bar{V}\right] = -\nabla p + \bar{J}\times\bar{B} + \mu\nabla^2\bar{V} - \frac{\mu}{K'}\bar{V} + g\beta T' \tag{2}$$

Energy Equation:

$$\rho C_p\left[\frac{\partial T'}{\partial t'} + (\bar{V}.\nabla)T'\right] = k\nabla^2 T' - \nabla q + \mu(\nabla u')^2 - Q_0 T' \tag{3}$$

Kirchhoff's First Law:

$$div\bar{J} = 0 \tag{4}$$

General Ohm's Law:

$$\bar{J} + \frac{\omega_e\tau_e}{B_0}(\bar{J}\times\bar{B}) = \sigma\left[\bar{E} + \bar{V}\times\bar{B} + \frac{1}{e\eta_e}\nabla p_e\right] \tag{5}$$

Gauss's Law of Magnetism:

$$div\bar{B} = 0 \tag{6}$$

Where $\bar{V}$ is the velocity vector, $\bar{\Omega}$ the angular velocity of the fluid, p the pressure, ρ the density, $\bar{B}$ the magnetic induction vector, $\bar{J}$ the current density, μ the coefficient of viscosity, t' the time, g the acceleration due to gravity, β the coefficient of volume expansion, K' is the permeability of the porous medium, C_p the specific heat at constant pressure, T' the temperature, T_∞ the reference temperature that of the left plate, k the

thermal conductivity, q the radiative heat , σ the electrical conductivity, B_0 the strength of the applied magnetic field, Q_0 the dimensional heat absorption coefficient, e the electron charge, ω_e the electron frequency, τ_e the electron collision time, p_e the electron pressure, $\bar{E}$ the electric field and η_e is the number density of electron.

3.2 FORMULATION OF THE PROBLEM

Consider an unsteady magneto hydrodynamic mixed convective flow of an electrically conducting, viscous, incompressible fluid through a porous medium bounded between two insulated infinite vertical plates in the presence of Hall current and thermal radiation. The plates are at a distance d apart. A Cartesian coordinate system with x' – axis oriented vertically upward along the centerline of the channel introduced. The z' – axis is taken perpendicular to the planes of the plates and is the axis of rotation and the entire system rotates about this axis with uniform angular velocity Ω'. The schematic diagram of the physical problem is shown in Figure 1. Since the plates of the channel are of infinite extent, all the physical quantities depend only on z' and t' only. The temperature $T'_w \cos\omega' t'$ of the right plate at $z' = d/2$ is considered to be varying periodically with time and the temperature $T' = T_0 = 0$ of the left plate at $z' = d/2$ is taken to be zero. Let (u', v', w') be the components of velocity in the directions (x', y', z') respectively. Since the plates are non – porous, therefore equation of continuity (1) on integration gives $w' = 0$. A strong transverse magnetic field of uniform strength B_0 is applied along the z' – axis. So, the equation (6) for the magnetic field $\bar{B} = (B'_x, B'_y, B'_z)$ gives $B'_z = B_0$ (constant).

If (J'_x, J'_y, J'_z) are the components of electric current density $\bar{J}$ then equation of conservation of electric charge in equation (4) gives J'_z = constant. For non – conducting plates

$$J'_z = 0 \tag{7}$$

at the plates and hence zero everywhere in the fluid. Under the usual assumptions that the electron pressure (for a weakly ionized gas), the thermoelectric pressure, ion slip and the

external electric field arising due to polarization of charges are negligible. It is assumed that no applied and polarization voltage exists. This corresponds to the case where no energy is being added or extracted from the fluid by electrical means (Meyer [14]). i.e., electrical field $\overline{E}=0$.

Therefore, the equation (5) takes the form:

$$\vec{J}+\frac{\omega_e\tau_e}{B_0}\left(\vec{J}\times\vec{B}\right)=\sigma\left(\vec{V}\times\vec{B}\right) \tag{8}$$

After using equation (7), equation (8) in component form becomes:

$$J_x'+\omega_e\tau_e J_y'=\sigma B_0 v' \tag{9}$$

$$J_y'-\omega_e\tau_e J_x'=-\sigma B_0 u' \tag{10}$$

Solving equations (9) and (10) for J_x' and J_y', we get

$$J_x'=\frac{\sigma B_0}{\left(1+m^2\right)}\left(mu'+v'\right) \quad \text{and} \quad J_y'=\frac{\sigma B_0}{\left(1+m^2\right)}\left(mv'-u'\right)$$

Where $m=\omega_e\tau_e$ is the Hall parameter. Under the foregoing assumptions and reference temperature $T_0=0$, Equation (2) in Cartesian components reduces to:

$$\frac{\partial u'}{\partial t'}=-\frac{1}{\rho}\frac{\partial p'}{\partial x'}+\upsilon\frac{\partial^2 u'}{\partial z'^2}+2\Omega' v'+\frac{\sigma B_0^2}{\rho\left(1+m^2\right)}\left(mv'-u'\right)-\frac{\upsilon}{K'}u'+g\beta T' \tag{11}$$

$$\frac{\partial v'}{\partial t'}=-\frac{1}{\rho}\frac{\partial p'}{\partial y'}+\upsilon\frac{\partial^2 v'}{\partial z'^2}-2\Omega' u'-\frac{\sigma B_0^2}{\rho\left(1+m^2\right)}\left(mu'+v'\right)-\frac{\upsilon}{K'}v' \tag{12}$$

and equation (3) becomes:

$$\rho C_p\frac{\partial T'}{\partial t'}=k\frac{\partial^2 T'}{\partial z'^2}-\frac{\partial q}{\partial z'}+\mu\left(\frac{\partial u'}{\partial z'}\right)^2-Q_0 T' \tag{13}$$

The boundary conditions for the flow problem are:

$$\left.\begin{aligned} u' = v' = T' = 0 \quad at \quad z' = -\frac{d}{2} \\ u' = v' = 0,\ T' = T'_w \cos\omega' t' \ at \quad z' = \frac{d}{2} \end{aligned}\right\} \tag{14}$$

Where T'_w is the mean temperature of the plate at $z' = d/2$ and ω' is the frequency of oscillation.

Following Cogley et al [5], the last term in the energy equation (13), $\frac{\partial q}{\partial z'} = 4\alpha^2 (T' - T_\infty)$ stands for radiative heat flux modifies to:

$$\frac{\partial q}{\partial z'} = 4\alpha^2 T' \tag{15}$$

in view of the reference temperature $T_\infty = 0$, where α^2 is the mean radiation absorption coefficient.

Introducing the following non dimensional quantities

$$\eta = \frac{z'}{d}, x = \frac{x'}{d}, y = \frac{y'}{d}, u = \frac{u'}{U}, v = \frac{v'}{U}, T = \frac{T'}{T'_w}, t = \frac{t'U}{d}, \omega = \frac{\omega' d}{U}, p = \frac{p'}{\rho U^2},$$
$$\mathrm{Re} = \frac{Ud}{\upsilon}, \Omega = \frac{\Omega' d^2}{\upsilon}, K = \frac{K'}{d^2}, Gr = \frac{g\beta d^2 T'_w}{\upsilon U}, Pe = \frac{\rho C_p dU}{k}, N = \frac{2\alpha d}{\sqrt{k}}, \tag{16}$$
$$M = \frac{\sigma\beta^2 d^2}{\rho\upsilon}, S = \frac{Q_o d}{\rho C_p U}, Ec = \frac{U^2}{C_p T'_w}$$

Using non – dimensional quantities from (16), the equations (11), (12) and (13) reduces to:

$$\frac{\partial u}{\partial t} = -\frac{\partial p}{\partial x} + \frac{1}{\mathrm{Re}}\frac{\partial^2 u}{\partial \eta^2} + \frac{2\Omega}{\mathrm{Re}} v + \frac{M(mv - u)}{\mathrm{Re}(1 + m^2)} - \frac{1}{K\,\mathrm{Re}} u + \frac{Gr}{\mathrm{Re}} T \tag{17}$$

$$\frac{\partial v}{\partial t} = -\frac{\partial p}{\partial y} + \frac{1}{\mathrm{Re}}\frac{\partial^2 v}{\partial \eta^2} - \frac{2\Omega}{\mathrm{Re}} u - \frac{M(mu + v)}{\mathrm{Re}(1 + m^2)} - \frac{1}{K\,\mathrm{Re}} v \tag{18}$$

$$\frac{\partial T}{\partial t} = \frac{1}{Pe}\frac{\partial^2 T}{\partial \eta^2} - \frac{N^2}{Pe}T - ST + (Ec)\left(\frac{\partial u}{\partial \eta}\right)^2 \tag{19}$$

Where U is the mean axial velocity, M the Magnetic parameter, Re the Reynolds number, Ω the rotation parameter, K the permeability of the porous medium, Gr the Grashoff number, Pe the Peclet number, N the Radiation parameter, S the Heat absorption parameter and Ec the Eckert number.

The corresponding transformed boundary conditions are:

$$\left.\begin{aligned} u = v = T = 0 \ at \ \eta = -\frac{1}{2} \\ u = v = 0, T = \cos\omega t \ \ at \ \eta = \frac{1}{2} \end{aligned}\right\} \tag{20}$$

For the oscillatory internal flow, we shall assume that the fluid flows only under the influence of a non dimensional pressure gradient oscillating in the direction of x' – axis only which is of the form $-\frac{\partial p}{\partial x} = P\cos\omega t$.

3.3 METHOD OF SOLUTION

By applying Galerkin finite element method for equation (17) over the element (e), $(\eta_l \le \eta \le \eta_k)$ is:

$$\int_{\eta_l}^{\eta_k}\left\{N^{(e)T}\left[\frac{\partial^2 u^{(e)}}{\partial \eta^2} - \mathrm{Re}\frac{\partial u^{(e)}}{\partial t} - Bu + P\right]\right\}d\eta = 0 \tag{21}$$

Where $P = Amv + 2\Omega v - \mathrm{Re}\frac{\partial p}{\partial x} + GrT$, $B = A + \frac{1}{K}$, $A = \frac{M}{1+m^2}$

Integrating the first term in equation (21) by parts one obtains

$$N^{(e)T}\left\{\frac{\partial u^{(e)}}{\partial \eta}\right\}_{\eta_l}^{\eta_k} - \int_{\eta_l}^{\eta_k}\left\{\frac{\partial N^{(e)I}}{\partial \eta}\frac{\partial u^{(e)}}{\partial \eta} + N^{(e)I}\left(\mathrm{Re}\frac{\partial u^{(e)}}{\partial t} + Bu^{(e)} - P\right)\right\}d\eta = 0 \tag{22}$$

Since the derivative $\frac{\partial u}{\partial \eta}$ is not specified at either ends of the element (e) $(\eta_i \le \eta \le \eta_k)$, so that neglecting the first term in equation (22), one gets:

$$\int_{\eta_i}^{\eta_k} \left\{ \frac{\partial N^{(e)'}}{\partial \eta} \frac{\partial u^{(e)}}{\partial \eta} + N^{(e)T} \left(\mathrm{Re} \frac{\partial u^{(e)}}{\partial t} + B u^{(e)} - P \right) \right\} d\eta = 0$$

Let $u^{(e)} = N^{(e)} \phi^{(e)}$ be the linear piecewise approximation solution over the element (e), $(\eta_i \le \eta \le \eta_k)$, where $N^{(e)} = [N_i \quad N_k]$, $\phi^{(e)} = [u_i \quad u_k]^T$ and $N_i = \frac{\eta_k - \eta}{\eta_k - \eta_i}$, $N_k = \frac{\eta - \eta_i}{\eta_k - \eta_i}$ are the basis functions. One obtains:

$$\int_{\eta_i}^{\eta_k} \left(\begin{bmatrix} N_i' N_i' & N_i' N_k' \\ N_k' N_i' & N_k' N_k' \end{bmatrix} \begin{bmatrix} u_i \\ u_k \end{bmatrix} \right) d\eta + \mathrm{Re} \int_{\eta_i}^{\eta_k} \left\{ \begin{bmatrix} N_i N_i & N_i N_k \\ N_i N_k & N_k N_k \end{bmatrix} \begin{bmatrix} \dot{u}_i \\ \dot{u}_k \end{bmatrix} \right\} d\eta + B \int_{\eta_i}^{\eta_k} \left\{ \begin{bmatrix} N_i N_i & N_i N_k \\ N_i N_k & N_k N_k \end{bmatrix} \begin{bmatrix} u_i \\ u_k \end{bmatrix} \right\} d\eta = P \int_{\eta_i}^{\eta_k} \begin{bmatrix} N_i \\ N_k \end{bmatrix} d\eta$$

Simplifying we get

$$\frac{1}{l^{(e)}} \begin{bmatrix} 1 & -1 \\ -1 & 1 \end{bmatrix} \begin{bmatrix} u_i \\ u_k \end{bmatrix} + \frac{\mathrm{Re}}{6} \begin{bmatrix} 2 & 1 \\ 1 & 2 \end{bmatrix} \begin{bmatrix} \dot{u}_i \\ \dot{u}_k \end{bmatrix} + \frac{B}{6} \begin{bmatrix} 2 & 1 \\ 1 & 2 \end{bmatrix} \begin{bmatrix} u_i \\ u_k \end{bmatrix} = \frac{P}{2} \begin{bmatrix} 1 \\ 1 \end{bmatrix}$$

where prime and dot denotes differentiation w.r.t η and time t respectively. Assembling the element equations for two consecutive elements $(\eta_{i-1} \le \eta \le \eta_i)$ and $(\eta_i \le \eta \le \eta_{i+1})$ following is obtained:

$$\frac{1}{l^{(e)}} \begin{bmatrix} 1 & -1 & 0 \\ -1 & 2 & -1 \\ 0 & -1 & 1 \end{bmatrix} \begin{bmatrix} u_{i-1} \\ u_i \\ u_{i+1} \end{bmatrix} + \frac{\mathrm{Re}}{6} \begin{bmatrix} 2 & 1 & 0 \\ 1 & 4 & 1 \\ 0 & 1 & 2 \end{bmatrix} \begin{bmatrix} \dot{u}_{i-1} \\ \dot{u}_i \\ \dot{u}_{i+1} \end{bmatrix} + \frac{B}{6} \begin{bmatrix} 2 & 1 & 0 \\ 1 & 4 & 1 \\ 0 & 1 & 2 \end{bmatrix} \begin{bmatrix} u_{i-1} \\ u_i \\ u_{i+1} \end{bmatrix} = \frac{P}{2} \begin{bmatrix} 1 \\ 2 \\ 1 \end{bmatrix} \quad (23)$$

Now put row corresponding to the node i to zero, from equation (23) the difference schemes with $l^{(e)} = h$ is:

$$\frac{1}{h^2}\left[-u_{i-1}+2u_i-u_{i+1}\right]+\frac{\mathrm{Re}}{6}\left[\dot{u}_{i-1}+4\dot{u}_i+\dot{u}_{i+1}\right]+\frac{B}{6}\left[u_{i-1}+4u_i+u_{i+1}\right]=P \qquad (24)$$

Applying the trapezoidal rule, following system of equations in Crank – Nicholson method are obtained:

$$A_1u_{i-1}^{n+1}+A_2u_i^{n+1}+A_3u_{i+1}^{n+1}=A_4u_{i-1}^{n}+A_5u_i^{n}+A_6u_{i+1}^{n}+12Pk \qquad (25)$$

Applying similar procedure to equations (18) and (19) the following equations are obtained:

$$B_1v_{i-1}^{n+1}+B_2v_i^{n+1}+B_3v_{i+1}^{n+1}=B_4v_{i-1}^{n}+B_5v_i^{n}+B_6v_{i+1}^{n}+12Qk \qquad (26)$$

$$C_1T_{i-1}^{n+1}+C_2T_i^{n+1}+C_3T_{i+1}^{n+1}=C_4T_{i-1}^{n}+C_5T_i^{n}+C_6T_{i+1}^{n}+(Ec)\left(\frac{\partial u_i'}{\partial \eta}\right)^2 \qquad (27)$$

Where $A_1=2\mathrm{Re}-6r+Bk$, $A_2=8\mathrm{Re}+12r+4Bk$, $A_3=2\mathrm{Re}-6r+Bk$, $A_4=2\mathrm{Re}+6r-Bk$,

$A_5=8\mathrm{Re}-12r-4Bk$, $A_6=2\mathrm{Re}+6r-Bk$, $B_1=2\mathrm{Re}-6r+Bk$, $B_2=8\mathrm{Re}+12r+4Bk$,

$B_3=2\mathrm{Re}-6r+Bk$, $B_4=2\mathrm{Re}+6r-Bk$, $B_5=8\mathrm{Re}-12r-4Bk$, $B_6=2\mathrm{Re}+6r-Bk$,

$C_1=2Pe-6r+(N^2+S)k$, $C_2=8Pe+12r+4(N^2+S)k$, $C_3=2Pe-6r+(N^2+S)k$,

$C_4=2Pe+6r-(N^2+S)k$, $C_5=8Pe-12r-4(N^2+S)k$, $C_6=2Pe+6r-(N^2+S)k$,

$$P=Amv_i'+2\Omega v_i'-\mathrm{Re}\frac{\partial p}{\partial x}+GrT_i',\ Q=Amu_i'+2\Omega u_i'+\mathrm{Re}\frac{\partial p}{\partial y};$$

Here $r=\frac{k}{h^2}$ and h, k are mesh sizes along η – direction and time – direction respectively. Index i refers to space and j refers to the time. In equations (25), (26) and (27) taking $i=1(1)n$ and using boundary conditions (20), then the following system of equations are obtained:

$$A_iX_i=B_i,\ i=1(1)3 \qquad (28)$$

Where A_i s are matrices of order n and X_i , B_i s are column matrices having n – components. The solutions of above system of equations are obtained by using Thomas algorithm for velocity, temperature and concentration. Also, numerical solutions for these equations are obtained by C – programme. In order to prove the convergence and stability of Galerkin finite element method, the same C – programme was run with smaller values of h and k and no significant change was observed in the values of u, v and T. Hence the Galerkin finite element method is stable and convergent.

Knowing the velocity field, the skin - friction at the plate in the dimensionless form is given by

$$\tau_1 = \left[\frac{\partial u}{\partial \eta}\right]_{\eta=0} \quad \text{and} \quad \tau_2 = \left[\frac{\partial v}{\partial \eta}\right]_{\eta=0} \tag{29}$$

Knowing the temperature field, the rate of heat transfer coefficient can be obtained which in non dimensional form, in terms of the Nusselt number is given by

$$Nu = -\left[\frac{\partial T}{\partial \eta}\right]_{\eta=0} \tag{30}$$

3.4 DISCUSSIONS OF THE RESULTS

In order to study the effect of different parameters appearing in the flow problem, we have carried out numerical calculations for the velocity field, temperature field, skin friction, and rate of heat transfer. To assess the effects of each parameter for small and large rotations, two values of the rotation parameter Ω (= 5 and 10) are considered.

Figure 2 shows the variation of velocity profiles under the influence of the rotation parameter Ω. The velocity decreases when Ω is increased. Figure 3 shows the variation of velocity with Reynolds number Re. It is evident from figure 3 that the increasing value of Re leads to increase of velocity. It is interesting to note that for large rotation the maximum of velocity no longer occurs at the centre of the channel but shifted towards the walls.

The variations of the velocity profiles with the Grashof number Gr are shown in Figure 4. For small rotations ($\Omega = 5$), the velocity increases with the increasing Grashof number. The maximum of the velocity profiles shifts towards right half of the channel due to the greater buoyancy force in this part of the channel due to the presence of hotter plate. For large rotation ($\Omega = 10$), the Grashof number has opposite effect on the velocity profiles in the right half and the left half of the channel. In the right half there lies hot plate at $\eta = 1/2$ and heat is transferred from the hot plate to the fluid and consequently buoyancy force enhances the flow velocity further. In the left half of the channel, the transfer of heat takes place from the fluid to the cooler plate at $\eta = 1/2$. Thus, the effect of Grashof number on the velocity is reversed i.e. velocity decreases with increasing Gr. It is evident from figure 5 that the velocity decreases with the increase of Hartmann number M. This is because of the reason that effects of a transverse magnetic field on an electrically conducting fluid gives rise to a resistive type force (called Lorentz force) similar to drag force and upon increasing the values of M increases the drag force which has tendency to slow down the motion of the fluid. Figure 6 shows the variation of the velocity with Hall parameter m. The velocity increases with the increase of m in the middle of the channel for small rotation ($\Omega = 5$) of the channel while for the large rotation ($\Omega = 10$) of the channel there is no significant effect of m on velocity (Figure 6).

The variation of the velocity profile with permeability of the porous medium K is shown in Figure 7. It is observed from Figure 7 that in the rotating channel the velocity decreases with increasing K. It is expected physically also because the resistance posed by the porous medium to the accelerated flow due to rotation reduces with increasing permeability K which leads to decrease in the velocity. For ($\Omega = 10$) velocity is much less than ($\Omega = 5$).

Figure 8 shows that with increasing Peclet number Pe the velocity decreases. The variation of velocity profile with radiation parameter N is shown in Figure 9. In the left half of the channel, the effect of N on the velocity is insignificant while in the right half of the channel velocity decrease with increase of N. It is evident from the Figure10 that the increasing pressure gradient P leads to the increase of velocity. Figure 11 shows the variation of the

velocity with frequency of oscillations ω. The velocity decreases with the increase of frequency of oscillations ω (Figure 11).

Figure 12 shows the variation of the velocity with Eckert number Ec. The velocity increases with the increase of Ec in the middle of the channel for small rotation ($\Omega = 5$) of the channel while for the large rotation ($\Omega = 10$) of the channel there is no significant effect of Ec on velocity (Figure 12). The variation of the velocity profile with heat absorption parameter S is shown in Figure 13. It is observed from Figure 13 that in the rotating channel the velocity decreases with increasing S. The temperature profile is shown in Figure 14. The temperature decreases with the increase of radiation parameter N, heat source S, the Peclet number Pe and the frequency of oscillations ω (Figure 14). It is interesting to note that the flow of heat is reversed with the increase of Peclet number Pe and viscous dissipation Ec.

Table 1. Skin – friction coefficients (τ_1 & τ_2)

Ω	Re	Gr	M	m	K	Pe	N	Ec	S	P	τ_1	τ_2
5	1	1	1	1	1	0.71	1	0.001	1.0	5	1.769	-0.591
10	1	1	1	1	1	0.71	1	0.001	1.0	5	2.310	-0.183
5	0.5	1	1	1	1	0.71	1	0.001	1.0	5	0.930	-0.606
5	1	3	1	1	1	0.71	1	0.001	1.0	5	1.941	-0.520
5	1	1	2	1	1	0.71	1	0.001	1.0	5	1.602	-0.681
5	1	1	1	3	1	0.71	1	0.001	1.0	5	1.907	-0.401
5	1	1	1	1	0.5	0.71	1	0.001	1.0	5	1.712	-0.653
5	1	1	1	1	1	7.0	1	0.001	1.0	5	1.755	-0.495
5	1	1	1	1	1	0.71	5	0.001	1.0	5	1.701	-0.684
5	1	1	1	1	1	0.71	1	0.100	1.0	5	1.824	-0.410
5	1	1	1	1	1	0.71	1	0.001	2.0	5	1.697	-0.604
5	1	1	1	1	1	0.71	1	0.001	1.0	10	3.501	-0.367

From table 1 we observed that the skin friction τ_1 decreases with increase of Peclet number Pe and Hartmann number M. The skin friction τ_1 increases with increase of rotation parameter Ω, Reynolds number Re, Grashof number Gr, Hall parameter m, Permeability of the porous medium K, Pressure gradient P. From table 1 we observed that the skin friction τ_2 decreases with increase of Peclet number Pe and Hartmann number M. The skin friction τ_2 increases with increase of rotation parameter Ω, Reynolds number Re, Grashof number Gr, Hall parameter m, Permeability of the porous medium K, Pressure gradient P.

Table 2. Rate of heat transfer

Pe	Ec	S	N	Nu
0.71	0.001	1.0	1.0	1.0329
7.0	0.001	1.0	1.0	1.1156
0.71	0.100	1.0	1.0	0.9647
0.71	0.001	2.0	1.0	0.9365
0.71	0.001	1.0	3.0	0.8941

From table 2 we observed that the rate of heat transfer decreases with increase of Eckert number Ec, heat source S and Radiation parameter N but increases with increase of Peclet number Pe.

OBSERVATIONS:

This work investigated the effect of thermal radiation and rotation on an unsteady magnetohydrodynamic mixed convection flow through a porous medium with hall current and heat absorption. The governing equations are approximated to a system of non linear partial differential equations by using Galerkin finite element method. The results are presented graphically and we can conclude that the flow field and the quantities of physical interest are significantly influenced by these parameters.

1. The velocity increases as rotation parameter Ω, Reynolds number Re, Grashof number Gr, Hall parameter m, Eckert number Ec and Pressure gradient P increases. However, the velocity was found to decreases as the Hartmann number M, Permeability of the porous medium K, Peclet number Pe, Heat absorption parameter S, Thermal radiation parameter N and Frequency of oscillation ω are increases.
2. The fluid temperature was found to decreases as the Heat absorption parameter S, thermal radiation parameter N and Peclet number Pe are increases. And it increases as Eckert number Ec increases.
3. The skin friction τ_1 decreases with increase of rotation parameter Ω, Heat absorption parameter S, Peclet number Pe Thermal radiation parameter N and Hartmann number M. However, it increases with increase of Reynolds number Re, Eckert number Ec, Grashof number Gr, Hall parameter m, Permeability of the porous medium K, Pressure gradient P.
4. The skin friction τ_2 decreases with increase of Peclet number Pe, Heat absorption parameter S, Thermal radiation parameter N and Hartmann number M. However it increases with increase of rotation parameter Ω, Reynolds number Re, Grashof number Gr, Hall parameter m, Eckert number Ec, Permeability of the porous medium K, Pressure gradient P.
5. The rate of heat transfer decreases as the Heat absorption parameter S, thermal radiation parameter N and Eckert number Ec are increases. And it increases as Peclet number Pe increases.

3.5 REFERENCES

[1] Alagoa K. D., Tay. G. and Abbey T. M. Radiation and free convection effects on a MHD flow through a Porous medium between infinite parallel plates with a time – dependent suction, *Astrophys. and space Sci.*, 260,455 (1999).

[2] Attia H. A. and Kotb N. A. MHD flow between two parallel plates with heat transfer, *Acta Mech*, 117,215 (1996).

[3] A.J. Chamkha, Unsteady MHD Convective Heat and Mass Transfer Past a Semi-infinite Vertical Permeable Moving Plate with Heat Absorption, *Int. J. Eng. Sci.*, 42, 217 – 230 (2004).

[4] Chang C. and Lundgren T. S., Duet flow in Magnetohydrodynamics, *Z. Angew. Math. Phys.*, 12, 100 – 114 (1961).

[5] Cogley A. C., Vincenti W. G., and Gilles S. E., Differential approximation for radiative transfer in a Non–grey gas near equilibrium, *American Institute of Aeronautics and Astronautics*, 6, 551 – 553 (1968).

[6] Crammer K. R. and Pai S. I., Magneto Fluid Dynamics for Engineers and Applied Physicists, *(McGraw-Hill Book Co. New York)*, 1973.

[7] Ferraro V. C. A. and Plumpton C., An Introduction to Magneto Fluid Mechanics, *(Clarendons Press, Oxford)*, 1966.

[8] Ghosh S. K., Beg O. A., and Narahari M., Hall effects on MHD flow in a rotating system with heat transfer characteristics, *Meccanica*, 44, 741(2009).

[9] Israel-Cookey C., Ogulu A. and Omubo-Pepple V. B., Influence of viscous dissipation on unsteady MHD free convective flow past an infinite heated vertical plate in porous medium with time dependent suction, *Int. J. Heat Mss Transfer*, 46,1253-1261(1972).

[10] Jain N. C., and Gupta P. Three dimensional free convection Couette flow with transpiration cooling, *Journal of Zhejiang University SCIENCE A*, 7(3), 340 – 346 (2006).

[11] Mazumder B. S., Gupta A. S. and Datta N., Flow and heat transfer in the hydromagnetic Ekman layer on a porous plate with Hall effects, *Int. J. Heat Mass Transfer*, 19, 523 – 527 (1976).

[12] Mazumder B. S., Gupta, A. S. and Datta N., Hall effects on combined free and forced convective hydromagnetic Flow through a channel, *Int. J. Engng. Sci.*, 14, 285 (1976).

[13] Mebine P., Radiation effects on MHD Couette flow with heat transfer between two parallel plates, *Global J Pure Appl. Math*, 3(2), 191 (2007).

[14] Meyer R. C., Magneto hypersonic rarefied flow at the stagnation point of a blunt body with slip and mass transfer, *J. Aerospace Sci.*, 25, 561 (1958).

[15] Ostrach, S., Combined natural and forced – convection Laminar flow and heat transfer of fluids with and without heat sources in channels with linearly varying wall temperatures, *NACATN*, 31 – 41(1954).

[16] Paul, T., Singh, A. K. and Mishra, A. K. *Journal of Math. Engg. in Industry*, 8, 177 (2001).

[17] Raptis A., Radiation and free convection flow through a porous medium, *Int. Commun. Heat Mass Transfer*, 25, 289 (1998).

[18] Sahin A., Three–Dimensional channel flows a porous medium, *Bulletin Calcutta Mathematical Society*, 101(5), 503 (2009).

[19] Satyanarayana P. V., and Venkataramana S. Hall current effect on magneto-hydrodynamics free-convection flow past a semi infinite vertical porous plate with mass transfer, S.V.University,Ph.D. Thesis, 2007.

[20] Shercliff, J. A., A Text Book of Magneto Hydrodynamics, *(Pergamon Press Ltd. New York)*, 1965.

[21] Singh K. D. and Rakesh Kumar, Combined effects of Hall Current and rotation on free convection MHD flow in a Porous channel , *Indian J Pure & Appl. Phys.*, 47, 617 – 623 (2009).

[22] Singh K. D. and Rakesh Kumar, Radiation effects on the exact solution of free convective oscillatory flow through porous medium in a rotating vertical channel, *J of Rajasthan Acad. Phy Sci*, 8(3), 295 – 310 (2009).

[23] Singh K.D. and Reena pathak, Effect of rotation and Hall current on mixed convection MHD flow through a porous medium filled in a vertical channel in presence of thermal radiation, *Indian J Pure & Appl. Phys.*, 50, 77-85 (2012).

[24] Sivaprasad R., Prasad Rao D. R. V. and Krishna D. V. Hall effects on unsteady MHD free and forced convection flow in a porous rotating channel, *Indian J. Pure Appl. Math.*, 19(7), 688 – 696 (1988).

[25] Soundalgekar V. M. and Upelkar A. G. Hall effects in MHD Couette flow with heat transfer, *IEEE Transactions on Plasma Sci.*, 14(5), 579 – 583 (1986).

[26] Yen T. and Chang C. Magnetohydrodynamic Coutte flow as affected by wall electrical conductances, *ZAMP*, 15, 400 (1964).

The contents of this chapter are published in International Journal of Mathematical Sciences, Technology and Humanities, 56(2012), pp. 593 – 615.

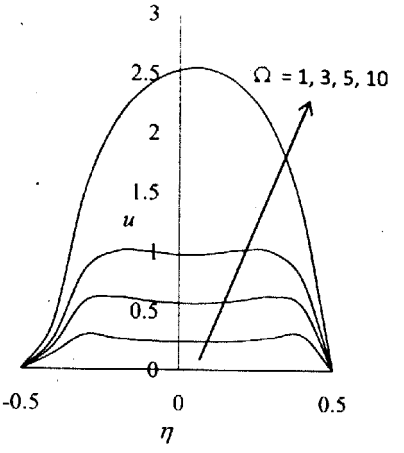

Figure 2. Variation of velocity profiles with Ω for Re = 1.0, Gr =1.0, M =1.0, m = 1.0, K = 1.0, Pe =0.71, N =1.0, P =5.0, Ec = 0.001, S = 1.0, ω =5.0 and t =1.0.

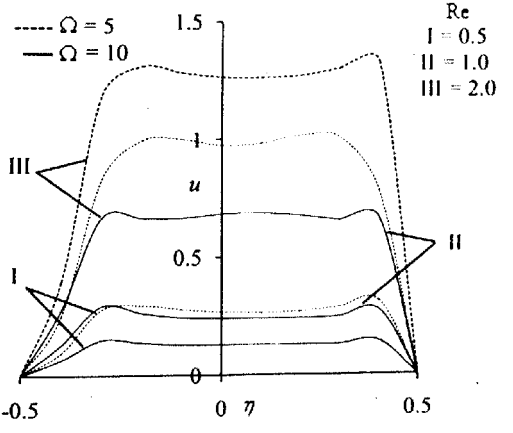

Figure 3. Variation of velocity profiles with Re for Gr =1.0, M =1.0, m = 1.0, K = 1.0, Pe =0.71, N =1.0, P =5.0, Ec = 0.001, S = 1.0, ω =5.0 and t =1.0.

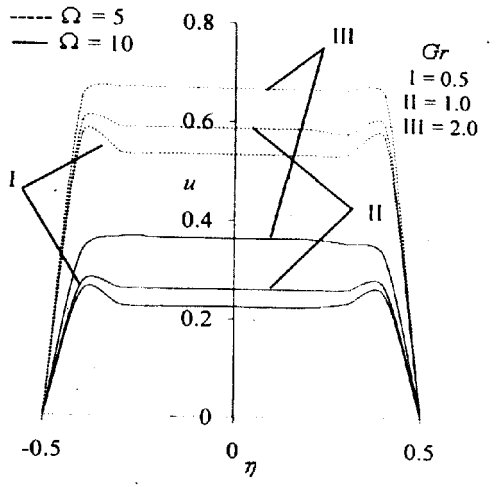

Figure 4. Variation of velocity profiles with Gr for Re =1.0, M =1.0, m = 1.0, K = 1.0, Pe =0.71, N =1.0, P =5.0, Ec = 0.001, S = 1.0, ω = 5.0 and t =1.0.

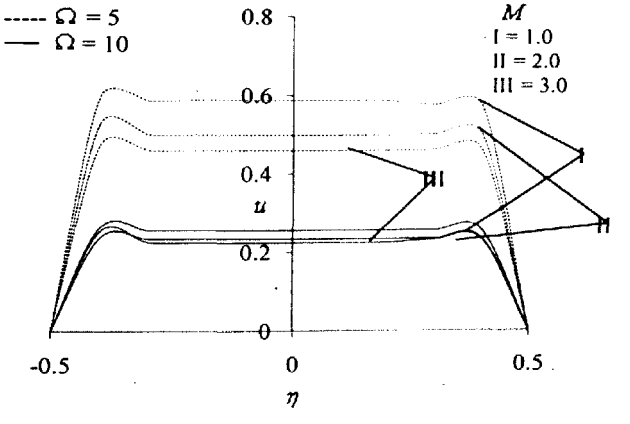

Figure 5. Variation of velocity profiles with M for Re =1.0, Gr =1.0, m = 1.0, K = 1.0, Pe =0.71, N =1.0, P =5.0, Ec = 0.001, S = 1.0, ω =5.0 and t =1.0.

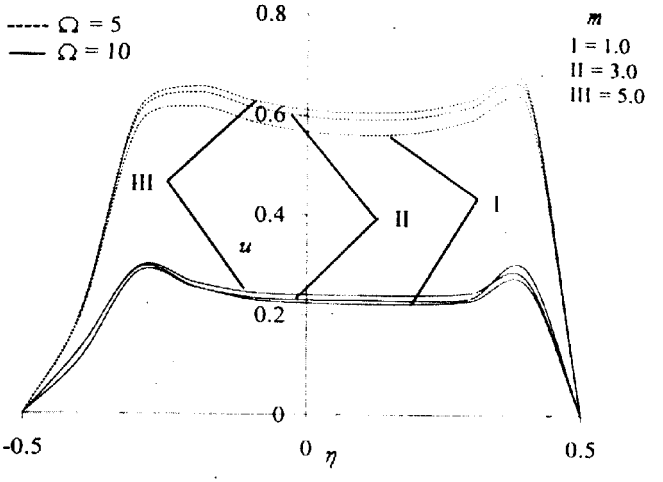

Figure 6. Variation of velocity profiles with m for Re = 1.0, Gr = 1.0, M = 1.0, K = 1.0, Pe = 0.71, N = 1.0, P = 5.0, Ec = 0.001, S = 1.0, ω = 5.0 and t = 1.0.

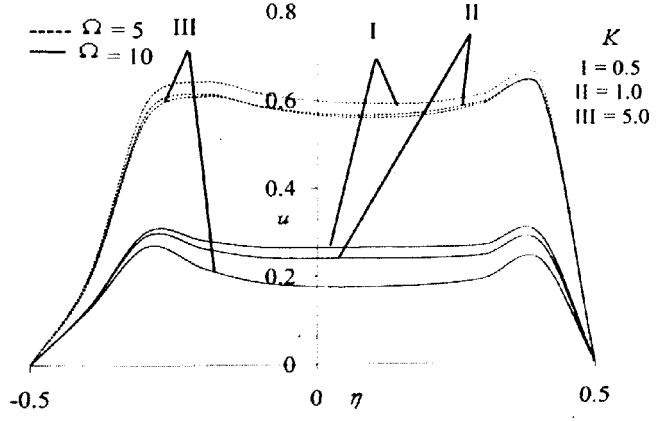

Figure 7. Variation of velocity profiles with K for Re = 1.0, Gr = 1.0, M = 1.0, m = 1.0, Pe = 0.71, N = 1.0, P = 5.0, Ec = 0.001, S = 1.0, ω = 5.0 and t = 1.0.

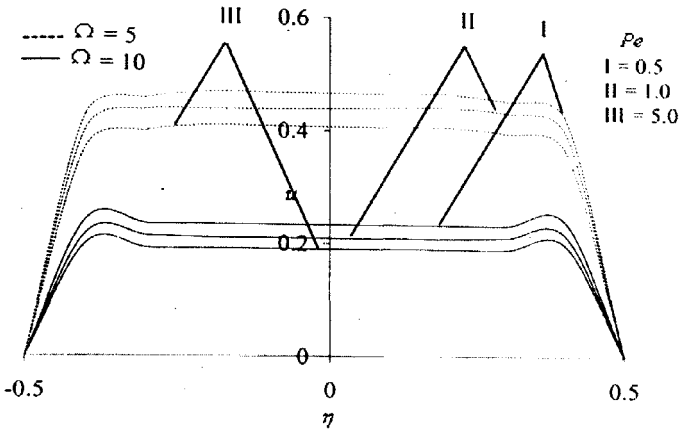

Figure 8. Variation of velocity profiles with Pe for Re = 1.0, Gr = 1.0, M = 1.0, m = 1.0, N = 1.0, K = 1.0, P = 5.0, Ec = 0.001, S = 1.0, ω = 5.0 and t = 1.0.

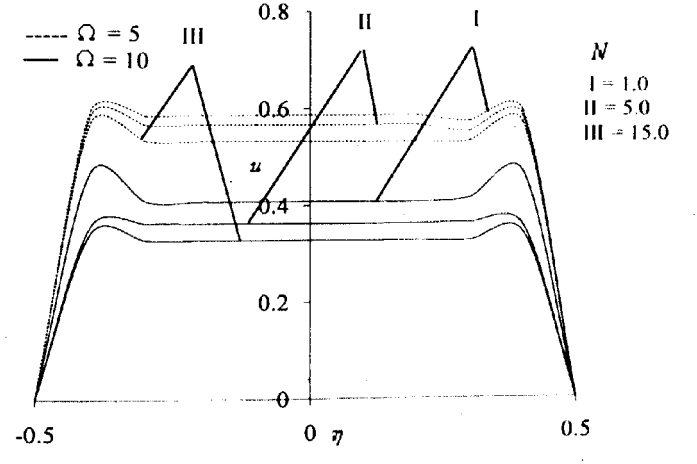

Figure 9. Variation of velocity profiles with N for Re = 1.0, Gr = 1.0, M = 1.0, m = 1.0, Pe = 0.71, K = 1.0, P = 5.0, Ec = 0.001, S = 1.0, ω = 5.0 and t = 1.0.

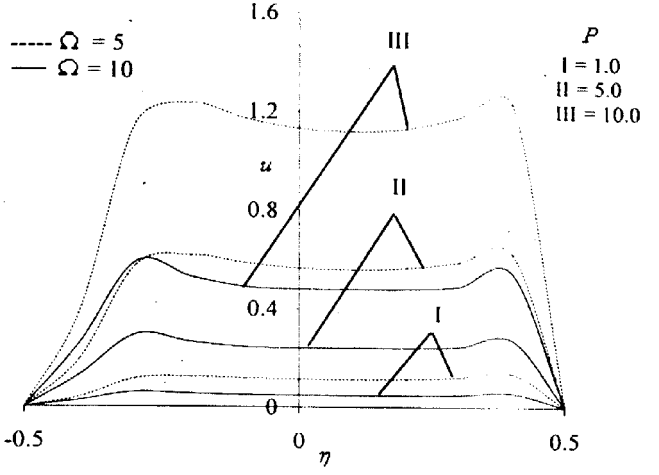

Figure 10. Variation of velocity profiles with P for Re = 1.0, Gr = 1.0, M = 1.0, m = 1.0, Pe = 0.71, K = 1.0, N = 1.0, Ec = 0.001, S = 1.0, ω = 5.0 and t = 1.0.

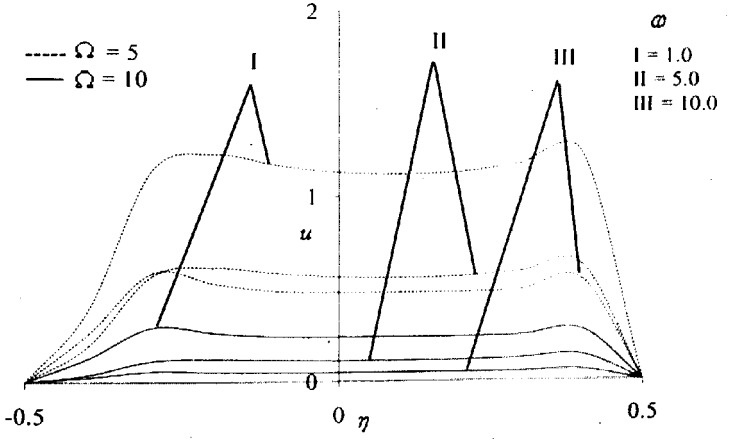

Figure 11. Variation of velocity profiles with ω for Re = 1.0, Gr = 1.0, M = 1.0, m = 1.0, Pe = 0.71, K = 1.0, N = 1.0, P = 5.0, Ec = 0.001, S = 1.0 and t = 1.0.

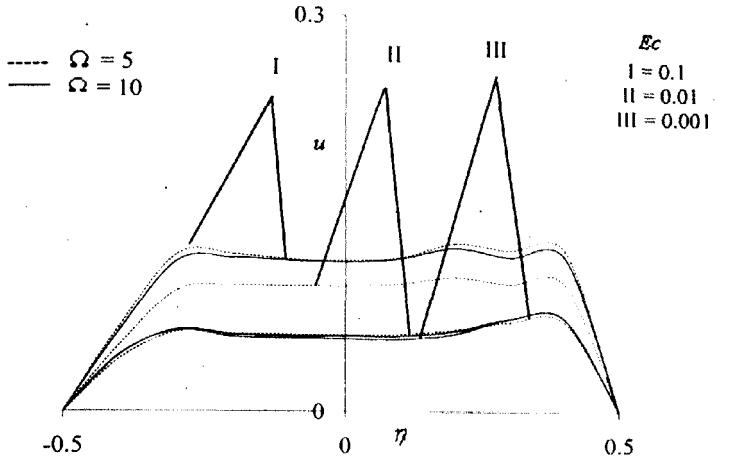

Figure 12. Variation of velocity profiles with Ec for Re = 1.0, Gr = 1.0, M = 1.0, m = 1.0, Pe = 0.71, K = 1.0, N = 1.0, P = 5.0, S = 1.0, ω = 5.0 and t = 1.0.

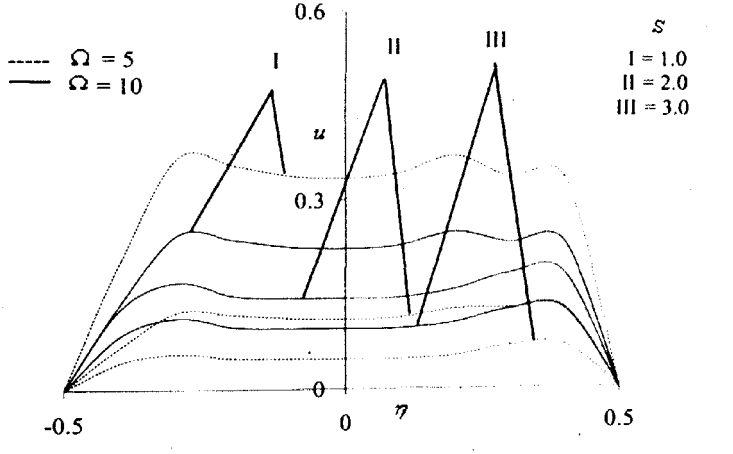

Figure 13. Variation of velocity profiles with S for Re = 1.0, Gr = 1.0, M = 1.0, m = 1.0, Pe = 0.71, K = 1.0, N = 1.0, P = 5.0, Ec = 0.001, ω = 5.0 and t = 1.0.

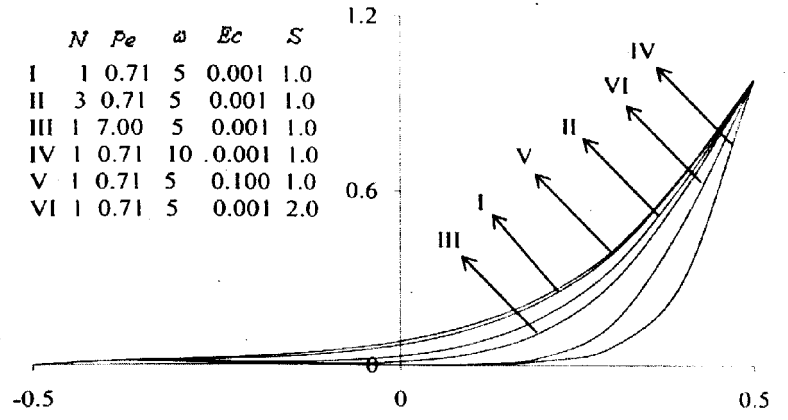

Figure 14. Variation of temperature profiles for $t = 1.0$.